

AD-A157 356

A Hybrid Mode and a Classification of Beam Plasma Instabilities

Y. Y. LAU

*Plasma Theory Branch
Plasma Physics Division*

July 11, 1985

This work was supported by the Office of Naval Research and the Defense Advanced Research Projects Agency (DoD), ARPA Order No. 4395, Amendment 41, monitored by the Naval Surface Weapons Center under Contract No. N60921-84-WR-W0131.



DTIC FILE COPY

NAVAL RESEARCH LABORATORY
Washington, D.C.

DTIC
ELECTE
JUL 19 1985
S D G

Approved for public release; distribution unlimited.

REPORT DOCUMENTATION PAGE				
1a REPORT SECURITY CLASSIFICATION UNCLASSIFIED		1b RESTRICTIVE MARKINGS		
2a SECURITY CLASSIFICATION AUTHORITY		3 DISTRIBUTION / AVAILABILITY OF REPORT Approved for public release; distribution unlimited.		
2b DECLASSIFICATION / DOWNGRADING SCHEDULE				
4 PERFORMING ORGANIZATION REPORT NUMBER(S) NRL Memorandum Report 5601		5. MONITORING ORGANIZATION REPORT NUMBER(S)		
6a. NAME OF PERFORMING ORGANIZATION Naval Research Laboratory	6b OFFICE SYMBOL (If applicable) Code 4790	7a. NAME OF MONITORING ORGANIZATION Naval Surface Weapons Center		
6c. ADDRESS (City, State, and ZIP Code) Washington, DC 20375-5000		7b. ADDRESS (City, State, and ZIP Code) Silver Spring, MD 20910		
8a. NAME OF FUNDING / SPONSORING ORGANIZATION DARPA	8b. OFFICE SYMBOL (If applicable)	9. PROCUREMENT INSTRUMENT IDENTIFICATION NUMBER		
8c. ADDRESS (City, State, and ZIP Code) Arlington, VA 22209		10. SOURCE OF FUNDING NUMBERS		
		PROGRAM ELEMENT NO. 62707E	PROJECT NO.	TASK NO.
				WORK UNIT ACCESSION NO. DN680-415
11 TITLE (Include Security Classification) A Hybrid Mode and a Classification of Beam Plasma Instabilities				
12. PERSONAL AUTHOR(S) Lau, Y.Y.				
13a. TYPE OF REPORT Interim	13b. TIME COVERED FROM _____ TO _____	14. DATE OF REPORT (Year, Month, Day) 1985 July 11	15 PAGE COUNT 40	
16 SUPPLEMENTARY NOTATION (See page ii)				
17 COSATI CODES			18 SUBJECT TERMS (Continue on reverse if necessary and identify by block number)	
FIELD	GROUP	SUB-GROUP		
			Beam plasma instabilities	
			Electron beam propagation	
19 ABSTRACT (Continue on reverse if necessary and identify by block number) We attempt to classify the interactions of an electron beam with a background plasma according to the beam energy and to the relative density of the beam and the plasma. Both the electron beam and the plasma are assumed to be cold, unmagnetized, collisionless, and all equilibrium self-fields have been assumed negligible. Emphasis is placed on the dynamical coupling of longitudinal and transverse motions as a result of relativistic and electromagnetic effects. Over many orders of magnitudes, we find that the parameter space may be divided into just a few domains, with different instability mechanisms. The boundaries separating these domains are given, together with the instability growth rates and the characteristic wave number of the instability within each of these domains. This classification thus provides and immediate assessment of the nature of the beam plasma interactions once fundamental parameters regarding the electron beam and the plasma are specified. In addition to the classical two stream instabilities and the Weibel type instabilities, a new mode, temporarily called the hybrid mode, is discovered: This hybrid mode is dominant when the electron beam is (Continues)				
20 DISTRIBUTION / AVAILABILITY OF ABSTRACT <input checked="" type="checkbox"/> UNCLASSIFIED/UNLIMITED <input type="checkbox"/> SAME AS RPT. <input type="checkbox"/> DTIC USERS		21. ABSTRACT SECURITY CLASSIFICATION UNCLASSIFIED		
22a NAME OF RESPONSIBLE INDIVIDUAL Y. Y. Lau		22b TELEPHONE (Include Area Code) (202) 767-2765	22c. OFFICE SYMBOL Code 4790	

16. SUPPLEMENTARY NOTATION (Continued)

This work was supported by the Office of Naval Research and the Defense Advanced Research Projects Agency (DoD), ARPA Order No. 4395, Amendment 41, monitored by the Naval Surface Weapons Center under Contract No. N60921-84-WR-W0131.

19. ABSTRACT (Continued)

highly relativistic. We provide several examples of current interest to demonstrate the use of this classification. The results have been tested against the dispersion relationship given by Tajima, Jones and Shoucri. Effects of a finite beam are discussed.

Accession For	
NTIS GRA&I	<input checked="" type="checkbox"/>
DTIC TAB	<input type="checkbox"/>
Unannounced	<input type="checkbox"/>
Justification	
By _____	
Distribution/	
Availability Codes	
Dist	Avail and/or Special
AI	



CONTENTS

I. INTRODUCTION	1
II. THE HYBRID MODE	4
III. A CLASSIFICATION OF BEAM PLASMA INSTABILITIES	9
IV. SOME EXAMPLES	17
V. DISCUSSIONS	20
ACKNOWLEDGMENT	22
APPENDIX — Hybrid Mode in a Finite Beam	31
REFERENCES	34

A HYBRID MODE AND A CLASSIFICATION OF BEAM PLASMA INSTABILITIES

I. Introduction

There is considerable renewed interest in the old subject of the electron stream interactions with plasmas. While the classical two stream instability is quite well-understood, much of the current effort has been placed on intense relativistic electron beams. Examples of areas of interest where such a study is warranted include: electron beam heating of a dense plasma for inertial confinement fusion driver;¹ laser-plasma beat wave acceleration of particles to ultra high energies;^{2,3} electron beam propagation under sub-atmospheric conditions^{4,5} and in the case of a modified betatron accelerator,⁶ the proposed method⁷ of injection and extraction of the electron beam by creating a plasma channel; etc.

The diverse areas mentioned above encompass a multi-dimensional parameter space which spans over many orders of magnitude. Depending on the objective of an investigation, a theoretical analysis of beam-plasma interaction is necessarily limited in scope, as the electromagnetic effects, the relativistic effects, and the coupling between the perpendicular and parallel motions, among different species of particles, compete with each other. In this paper, we attempt to classify various beam-plasma instabilities⁸⁻¹² according to the electron beam energy and the electron beam density (relative to the background plasma density). Domains of instability mechanisms are determined, within each of which the instability growth rate and the minimum axial wavelengths for the instabilities are displayed. Such a classification then provides an

immediate determination of the nature and the importance of a particular instability, once the beam energy, the beam density, and the background plasma density are given. This would allow more ready refinement of the theory, if necessary, as the dominant physical mechanisms are isolated in such a classification.

During our survey of the parameter space, we identified an instability, which we termed a hybrid instability. This instability is important for the propagation of a long, thin relativistic electron beam into a tenuous background of ions. The phase (and group) velocity of the wave along the beam, in the laboratory frame, is $1/2$ of the speed of light. The growth rate is proportional to the quarter powers of the electron density and of the ion density, and inversely to the quarter powers of beam energy and of the ion mass.

The hybrid instability could be important in the "ion focus regime", where an intense electron beam propagates in a plasma channel, which is either preformed or self-generated. If the plasma channel is tenuous, the beam electrons electrostatically eject the plasma electrons from the beam path, leaving behind the plasma ions which then guide the beam electrostatically. An example where this hybrid instability is possibly a dominant one, is when a preformed plasma channel is generated to extract an electron beam in a modified betatron configuration, after the electron beam is fully accelerated. (See examples below).

In this paper, we shall first present a simple physical argument which leads to the dispersion relationship of the hybrid mode for a slab model. It turns out that the simple dispersion relationship thus derived is an excellent approximation to the full dispersion relationship,¹⁰⁻¹² which incorporates all electromagnetic and relativistic effects. We find that the dispersion

relationship is also applicable to a cylindrical beam of small, but finite cross sections [see Appendix].

To place the hybrid mode in a proper perspective, in Section III we provide the classification scheme, based on the beam energy and beam density. This classification identifies the domains for the hybrid mode, the Weibel mode,¹³ and the classical two stream instabilities. In that section, we also furnish a simple derivation of the Weibel mode for a relativistic electron beam. The growth rates and the minimum axial wavelengths for the various instabilities are catalogued for easy reference. Several examples of current interest are given in Section IV to demonstrate the ready utilization of the classification scheme established in Section III.

The basic assumptions are now stated. We assume that the external magnetic field is unimportant. This is certainly true in the ion focus regime mentioned above. The plasma and the beam are assumed collisionless. The plasma is at rest, and both the plasma and the beam are cold. It is assumed that there is no plasma return current. One may argue that such an assumption is valid in the ion focus regime where the background plasma density is low. The classification is based on a model of infinite uniform beam plasma system. The latter assumption is relaxed in the Appendix. In fact, if $k_{\perp}^2 \sim 1/r_b^2 \gg k^2$ where k_{\perp} is the perpendicular wave number, k is the axial wave number and r_b is the electron beam radius, the slab model provides an adequate description for global modes of a sharp boundary model if $k_{\perp} r_b$ is taken as a suitably quantized number greater than unity in order of magnitude.^{10,11} It is within this context that our classification of instabilities is made. We shall further discuss these basic assumptions, and the limitations they impose, in the last section.

II. The Hybrid Mode

The dispersion relationship for the hybrid mode, together with the physical picture, is now presented. For simplicity, we consider a one-dimensional model. The approach is very similar to the one used to describe simple plasma oscillations.

Consider an infinitely uniform electron beam propagating in the z -direction with constant velocity v_0 . The beam is highly relativistic, i.e.,

$$\gamma \gg 1 \quad (1)$$

where $\gamma = (1 - v_0^2/c^2)^{1/2}$ is the relativistic mass factor and c is the speed of light. The beam is cold and is embedded in a uniform background of ions of considerably lower density. The ions, of mass m_i , are also cold and are motionless in equilibrium. We assume that there is a force balance for the ions and for the electrons in equilibrium. For the electrons the almost perfect cancellation between the self electric field and the self magnetic field, (for $\gamma \gg 1$) together with the weak ionic background, would make a perfect equilibrium of cold electronic flow plausible. For the ions, because of their mass, we simply ignore whatever ionic motions which may have resulted from the equilibrium electric field. If the characteristic time of the instability is short compared with the free-fall time of the ions, one may then ignore the external forces on the ions in the equilibrium states, to the lowest approximation. This in fact can be shown to be the case through a Vlasov description of the ionic responses. The effects of these equilibrium ion motions may then be evaluated in a qualitative manner by, for example, pretending that there is a "temperature" of the ions for the equilibrium. Here, we just assume, for convenience, that such temperature is zero. Simply stated, we assume that the unperturbed equilibrium fields are unimportant.

This is certainly true in the hypothetical situation of a completely neutralized beam and plasma. The above, then, constitutes the working hypothesis.

To consider the small signal stability of such a beam-plasma system, we focus mainly on the transverse motion of the beam since a beam electron is more responsive to a transverse force than to a longitudinal force when the beam is highly relativistic. Let ξ_e be the electron displacement, from its equilibrium position, in the transverse direction, and ξ_i be the ion displacement, also in the transverse direction [Fig. 1]. These displacements then generate AC electric fields E_{1e} and E_{1i} , and AC magnetic fields B_{1e} and B_{1i} . Here the subscripts e and i are used to denote that part of electric field (or magnetic field) which is due to ξ_e and ξ_i , respectively. Thus

$$E_{1e} = 4\pi|e|n_b\xi_e, \quad E_{1i} = -4\pi|e|n_p\xi_i \quad (2)$$

$$B_{1e} = -E_{1e}v_0/c, \quad B_{1i} = 0 \quad (3)$$

where n_b and n_p are, respectively, the beam electron and plasma ion density in equilibrium and e is the electron charge. Here we assume that the ions are singly ionized.

Equation (2) is obvious. B_{1e} as given by Eq. (3) may easily be obtained by visualizing the dipole current layers labeled O and E in Fig. 1. Since there is no unperturbed ion motion, $B_{1i} = 0$, as shown in Eq. (3).

The linearized equations of motions for the electrons and ions then read

$$\gamma m_e \ddot{\xi}_e = -|e| [E_{1e} + E_{1i} + \frac{v_0}{c} \times (B_{1e} + B_{1i})] \quad (4)$$

$$m_i \ddot{\xi}_i = + |e| [E_{1e} + E_{1i}]. \quad (5)$$

Since we assume that there is no ionic motion in equilibrium, the Lorentz force is absent for the ions [cf. Eq. (5)]. Further simplification is possible by using Eq. (1) and by the assumption that the background plasma is tenuous. By Eq. (1), $E_{1e} + (v_0/c) \times B_{1e} = 0$ since the self electric field and the self magnetic field generated by the electronic dipole layer cancelled to order $1/\gamma^2$, and γ is large [cf. Fig. 1; also, Eqs. (2), (3)]. The latter assumption permits us to ignore E_{1i} in comparison with E_{1e} in Eq. (5). Thus, Eqs. (4) and (5) are simplified to read

$$\gamma_0 m_e \ddot{\xi}_e = - |e| E_{1i} = 4\pi |e|^2 n_p \xi_i \quad (6)$$

$$m_i \ddot{\xi}_i = + |e| E_{1e} = + 4\pi |e|^2 n_0 \xi_e. \quad (7)$$

For a perturbation with dependence $\exp(i\omega t - ikz)$, $\ddot{\xi}_e = -(\omega - kv_0)^2 \xi_e$ and $\ddot{\xi}_i = -\omega^2 \xi_i$. Using these expressions in Eqs. (6) and (7) and multiplying the resultant equations, we obtain the dispersion relationship for the hybrid mode

$$\omega^2 (\omega - kv_0)^2 = \omega_p^2 \omega_{b\perp}^2 \quad (8)$$

where

$$\omega_p^2 = 4\pi e^2 n_p / m_i \quad (9)$$

$$\omega_{b\perp}^2 = 4\pi e^2 n_0 / m_e \gamma. \quad (10)$$

The instability growth rate may readily be obtained from a square root of Eq. (8):

$$\omega = \frac{1}{2} kv_0 \pm i \left(\omega_p \omega_{b\perp} - \frac{1}{4} k^2 v_0^2 \right)^{1/2}. \quad (11)$$

This dispersion relationship has been shown to be an excellent approximation to that for a thin beam which is highly relativistic ($\beta \approx 1$). The latter is given by Eq. (A11) of the Appendix. The solution to Eq. (A11) is slightly more general than (11) and is sketched in Fig. 2, where the real part ω_r and the imaginary part ω_i are shown. In Fig. 2, $n \equiv \omega_{b\parallel}^2 / \omega_p^2 \equiv \omega_{b\perp}^2 / \gamma^2 \omega_p^2$. Equation (A11) reduces to Eq. (11) in the limit $\beta = 1$.

Several points for the hybrid mode are noteworthy: (a) The phase and group velocity of the unstable waves equal to $v_0/2 \approx c/2$. (b) The instability is absent if the axial wavelength λ satisfies the inequality

$$\lambda = \frac{2\pi}{k} < \frac{\pi c}{\sqrt{\omega_p \omega_{b\perp}}} \equiv \lambda_H \equiv \frac{2\pi}{k_H}. \quad (12)$$

Here, we have used a subscript H to denote the critical axial wavelength for the hybrid mode. (c) The instability growth rate, for $k \ll k_H$, is given by

$$\omega_i = \omega_{iH} \equiv \sqrt{\omega_p \omega_{b\perp}} \quad (13)$$

which is independent of k_{\perp} and of k . (d) We may more precisely state what we meant by a "tenuous" ionic background. For $|E_{1i}| \ll |E_{1e}|$, as we have assumed in deriving (7) from (5), we must have $n_b |\xi_e| \gg n_p |\xi_i|$ [cf. (2)]. This inequality becomes

$$\omega_{b\perp}^2/\omega_p^2 \gg 1 \quad (14)$$

if we use $\omega^2 = -\omega_p\omega_{b\perp}$ in (7). (e) While the dispersion relationship (11) is independent of k_\perp , the transverse displacement is extremely important. An analogous example would just be the simple plasma dispersion relation $\omega^2 = \omega_p^2$, which is independent of \vec{k} (but displacements of particles parallel to \vec{k} are important).

At the risk of some redundancy, we paraphrase the above derivation for the hybrid mode by a physical description of the instability mechanism, as depicted in the sequence of events in Fig. 3. Suppose that a sheet of electrons, whose unperturbed position is on the sheet labeled 0 as shown in Fig. 3(a), is displaced to position labeled E, at a distance ξ_e from 0. Assume also that a sheet of ions is displaced to level I, by a distance ξ_i from 0. Let $\xi_i > \xi_e$ as shown in Fig. 3(a). If the electron beam is highly relativistic, the force on the electron sheet E is due only to the electric field E_{1i} generated by the ion sheet I, since the self electric field E_{1e} and the self magnetic field B_{1e} , which are generated by the dipole sheets E and 0, are canceled to order $1/\gamma^2$. Thus sheet E is accelerated toward sheet I, due only to the ionic electric field.

Now consider the forces on the ion sheet I in Fig. 3(a). Sheet I is not acted on by the electrons at all, since the electric field E_{1e} and magnetic field B_{1e} (generated by ξ_e) are confined within the region between E and 0. (One may visualize this by imagining sheet E and 0 as capacitor plates, which generate E_{1e} , and also as a dipole sheet current, which generated B_{1e}). Thus sheet I is subject only to its own restoring force E_{1i} . However, since the ion background is tenuous, E_{1i} is small. In other words, the ion sheet I in Fig. 3(a) is not subject to any perturbed force, to the lowest order. Since E

is accelerated toward I, as explained in the previous paragraph, E overtakes I at a later time, as shown in Fig. 3(b).

In Fig. 3(b), $\xi_e > \xi_i$. Now sheet E is not subject to any perturbed force, to the order we are considering, since E_{1e} and B_{1e} canceled to order $1/\gamma^2$, and E_{1i} is confined only within I and O. Thus once E surpasses I, as in Fig. 3(b), E moves with a constant velocity. However, I is accelerated toward E, because of E_{1e} (again, E_{1i} is small because of the low background ion density). Thus, at a later time I overtakes E, as shown in Fig. 3(c), and the whole sequence repeats. Thus the electron sheet E and the ion sheet I gradually deviate from their original position O, and this is essentially the basic mechanism which drives the hybrid mode.

The above physical description is in some respect similar to the one given for simple plasma oscillations ($\omega = \omega_p$). For example, the argument does not require a detailed specification of the wave numbers, of the beam and plasma dimensions and of the profiles. One may then be tempted to conclude that the hybrid instability is a fundamental one as long as $\gamma_0 \gg 1$ and $\omega_{b\perp}^2/\omega_p^2 \gg 1$. In fact, we shall show in the Appendix that essentially the same dispersion relationship (8), or (11), is obtained for a cylindrical beam with a sharp boundary profile.

We postpone to the next two sections for a discussion of the relationship of this hybrid mode and other beam-plasma instabilities.

III. A Classification of Beam Plasma Instabilities

To place the hybrid mode in the "general picture" of beam plasma interactions, we have conducted a limited search of the literature in which the relativistic and electromagnetic effects have been treated. We found that the recent work of Tajima,¹⁰ Jones,¹¹ and Shoucri¹² are the closest to the

present one. The studies of Jones and Tajima are more general, as they included bounded systems in cylindrical geometries. Their results firmly establish the validity of the use of a slab model, if the beam radius r_b (or thickness τ) is sufficiently small, and if the perpendicular wave number k_{\perp} in the slab model is to be replaced by p/r_b , where p is a quantized number of order unity, (or larger for higher radial modes). Shoucri¹² considered only a slab geometry, but he brought out an interesting point regarding the coupling of electromagnetic and relativistic effects. We postpone to Section V for a brief discussion of other literature.

The three authors mentioned in the previous paragraph produced, among other things, the same dispersion relationship. For example, the dispersion relationship given in Eq. (20) of Shoucri¹² is equivalent to the dispersion relationship (40) of Tajima,¹⁰ which is in turn equivalent to that given in p. 1931 of Jones,¹¹ who also noted such a correspondence. This dispersion relationship, for the slab model, reads

$$B E = C \quad (15)$$

where

$$B = 1 - \omega_p^2/\omega^2 - \omega_{b11}^2/\Omega^2 \quad (16)$$

$$E = 1 - k_{\perp}^2 c^2/\omega^2 - k_{\perp}^2 c^2/\omega^2 - (\omega_p^2 + \omega_{b\perp}^2)/\omega^2 \quad (17)$$

$$C = k_{\perp}^2 c^2 \omega_p^2 (\omega_{b11}^2 - \omega_{b\perp}^2)/\omega^2 \Omega^2. \quad (18)$$

Here, B represents the classical beam plasma interaction, E the electromagnetic mode, and C the coupling of the two. In Eqs. (16)-(18), ω

is the frequency, k is the axial wave number, k_{\perp} is the perpendicular wave number, $\Omega = \omega - kv_0$, ω_p is the plasma frequency of the background, $\omega_{b\perp}^2 = 4\pi e^2 n_b / m_e \gamma$, and $\omega_{b\parallel} = \omega_{b\perp} / \gamma$. Note from Eq. (18) that $C = 0$ if $k_{\perp} = 0$, or if $\omega_p = 0$, or in the non-relativistic limit, in which case $\omega_{b\parallel} = \omega_{b\perp}$. Since the dispersion relation (15) is derived under the assumption that the unperturbed force on each of the particle species is negligible, hereafter ω_p may stand for ω_{pi} or ω_{pe} depending on the case of interest.

The dispersion relationship (15) $D(\omega, \vec{k}) = BE - C = 0$, in the limit $k_{\perp} - 1/r_b \gg k$, is characterized just by two dimensionless parameters: $\beta \equiv v_0/c$ and $\eta \equiv \omega_{b\parallel}^2 / \omega_p^2$. The first parameter reflects the beam energy (E_b) and η the density ratio of the beam and the background plasma. This can be seen by normalizing all frequencies with respect to ω_p , and all wave numbers with respect to ω_p/v_0 . It is for this reason that we are able to classify the beam plasma instability according to just two parameters β and η , over a wide range as discussed below.

Extensive numerical and analytical studies of the dispersion relationship (15) lead to the classification shown in Fig. 4. In this figure, the $\eta - E_b$ plane is divided into five domains. In each of these domains, the growth rates of the instability scale differently but the instability mechanism can be described simply. For example, the hybrid mode examined in the previous section falls in Domain V of Fig. 4. We shall now document the approximate growth rates for these domains. We should also point out that the boundaries between the domains are not sharp. The main use of this classification is then to provide an immediate determination of the instability of a given system, once the beam energy and the background plasma densities are given.

Some examples will be given in the next section. In all these examples, the approximate formulas given below have been favorably compared with the full dispersion relationship (15).

(A) $\beta\gamma < 1$ (i.e., $E_b < 212$ keV).

If $\beta\gamma < 1$, the beam is essentially non-relativistic. In this case, $C = 0$ in (15), and the dispersion relationship for the classical two-stream instability

$$1 - \frac{\omega_p^2}{\omega^2} - \frac{\omega_{b11}^2}{\Omega^2} = 0 \quad (19)$$

is readily recovered from (15), regardless of the value of k_{\perp} . We subdivide into two cases: $\eta = \omega_{b11}^2/\omega_p^2 < 1$ and $\eta > 1$.

(A1) $\eta < 1$ (DOMAIN I)

In this case, the background plasma density much exceeds the beam density. This is the typical case treated in most text books. The dispersion diagram is shown in Fig. 5. According to (19), the peak growth rate $\omega_i(\max)$, the cutoff wave number k_c , and ω_r are given by

$$\omega_i(\max) = \omega_p(\sqrt{3}/2) (\eta/2)^{1/3} = 0.687\eta^{1/3}\omega_p \quad (20a)$$

$$k_c = (\omega_p/v_o)[1 + (3/2)\eta^{1/3}] \quad (20b)$$

$$\omega_r = kv_o. \quad (20c)$$

This instability is absent for $k > k_c$. The case (A1) is labeled as I in Fig. 4; the dominant instability being the weak beam classical two stream instability.

(A2) $\eta > 1$. (DOMAIN II)

In this case, the background plasma has a lower density than the beam. The dispersion relationship (19) may also be analyzed using the standard technique. The dispersion diagram is sketched in Fig. 6. The peak growth rate, $\omega_i(\text{max})$, the cutoff wave number k_c , and ω_r for the unstable mode are:

$$\omega_i(\text{max}) = 0.687 \omega_p \eta^{1/6} \quad (21a)$$

$$k_c = (\omega_p/v_o) [\eta^{1/2} + (3/2)\eta^{1/6}] \quad (21b)$$

$$\omega_r = (kv_o)/\eta. \quad (21c)$$

The scalings given in (21) are quite different from those in (20). Note, however, that (20) and (21) yield the same result if $\eta = 1$. Equations (21) characterize the parameter space labeled II in Fig. 4, where the beam dominated classical two stream instability is prevalent.

The dispersion relationship (19) is well-known. It is unnecessary to furnish here a simple physical picture to support the derivation of (19). We now turn to the case where the relativistic effects are important.

(B) $\beta\gamma > 1$ (i.e., $E_b > 212$ keV).

When the beam energy is sufficiently high, the relativistic effects, the electromagnetic effects, and parallel and transverse motions are all coupled.

For $\beta\gamma > 1$, we may subdivide into three domains according to $\eta < 1/\beta^2\gamma^2$, $1/\beta^2\gamma^2 < \eta < \beta^2\gamma^2$, and $\eta > \beta^2\gamma^2$. These three domains are labeled III, V, IV, respectively. The approximate dispersion relationships, together with the growth rates and k_c , for each of these domains are displayed as follows.

$$(B1) \quad \eta < 1/\beta^2\gamma^2 \quad (\text{DOMAIN III})$$

This case corresponds to a tenuous relativistic electron beam embedded in a dense background plasma. Extensive numerical solution to (15) suggests that, in this case, we may approximate $B = 1 - \omega_p^2/\omega^2$, $E = - (k_{\perp}^2 c^2 + \omega_p^2 + \omega_{b\perp}^2)/\omega^2$ and $C = - \beta^2 k_{\perp}^2 c^2 \omega_p^2 \omega_{b\perp}^2 / \omega^2 \Omega^2$. Then Eq. (15) yields

$$1 - \frac{\omega_p^2}{\omega^2} = \left\{ \frac{k_{\perp}^2 c^2}{k_{\perp}^2 c^2 + \omega_p^2 + \omega_{b\perp}^2} \right\} \frac{\beta^2 \omega_p^2 \omega_{b\perp}^2}{\omega^2 \Omega^2} \quad (22)$$

which, in the limit $k_{\perp}^2 c^2 \gg \omega_p^2 + \omega_{b\perp}^2$, reduces to

$$1 - \frac{\omega_p^2}{\omega^2} = \frac{\beta^2 \omega_p^2 \omega_{b\perp}^2}{\omega^2 \Omega^2}. \quad (22a)$$

If we normalize $\bar{\omega} = \omega/\omega_p$, $\bar{\Omega} = \Omega/\omega_p$, Eq. (22a) may be written as

$$1 - \frac{1}{\bar{\omega}^2} = \frac{\beta^2 \gamma^2 \eta}{\bar{\omega}^2 \bar{\Omega}^2} \quad (22b)$$

where the parameter $\beta^2 \gamma^2 \eta$ enters. Recall that we have in this subsection assumed $\beta^2 \gamma^2 \eta < 1$.

The dispersion curve according to (22) is sketched in Fig. 7. The maximum growth rate $\omega_i(\text{max})$, the critical k_c , and ω_r are given by

$$\omega_i(\text{max}) = 0.687 (\beta^2 \gamma^2 \bar{\eta})^{1/3} \omega_p \quad (23a)$$

$$k_c = (\omega_p/v_0) [1 + (3/2)(\beta^2 \gamma^2 \bar{\eta})^{1/3}] \quad (23b)$$

$$\omega_r = kv_0. \quad (23c)$$

In (23a) and (23b),

$$\bar{\eta} = \eta \left[\frac{k_{\perp}^2 c^2}{k_{\perp}^2 c^2 + \omega_p^2 + \omega_{b\perp}^2} \right], \quad (24)$$

which reduces to η in the limit $k_{\perp}^2 c^2 \gg \omega_p^2 + \omega_{b\perp}^2$. Note from Fig. 7 that as $k \rightarrow 0$, $\omega_i \rightarrow \beta \gamma \sqrt{\bar{\eta}} \omega_p$, which is non-zero. This mode has been called a Weibel mode,^{13,14} and is predominant in Domain III in the classification shown in Fig. 4.

$$(B2) \quad \eta > \beta^2 \gamma^2 \quad (\text{DOMAIN IV})$$

This limit is the opposite as the case (B1). [cf. replace η by $1/\eta$]. In this limit we may approximate $B = 1 - \omega_{b\perp}^2/\Omega^2$, $E = - (k_{\perp}^2 c^2 + \omega_p^2 + \omega_{b\perp}^2)/\omega^2$, $C = - \beta^2 k_{\perp}^2 c^2 \omega_p \omega_{b\perp}^2 / \omega^2 \Omega^2$, and (15) becomes

$$1 - \frac{\omega_{b\perp}^2}{\Omega^2} = \left(\frac{k_{\perp}^2 c^2}{k_{\perp}^2 c^2 + \omega_p^2 + \omega_{b\perp}^2} \right) \frac{\beta^2 \omega_p \omega_{b\perp}^2}{\omega \Omega^2}. \quad (25)$$

For simplicity, we further assume $k_{\perp}^2 c^2 \gg \omega_p^2 + \omega_{b\perp}^2$ to reduce (25) to an even simpler form which is independent of k_{\perp} :

$$1 - \frac{\omega_{b\perp}^2}{\Omega^2} = \frac{\beta^2 \omega_p \omega_{b\perp}^2}{\omega \Omega^2}. \quad (26)$$

The solution to (26) is sketched in Fig. 8; the maximum growth rate $\omega_i(\max)$, k_c , and ω_r are given by

$$\omega_i(\max) = 0.687 \omega_p (\beta\gamma)^{2/3} n^{1/6} \quad (27a)$$

$$k_c = (v_o/\omega_p) [n^{1/2} + (3/2)(\beta\gamma)^{2/3} n^{1/6}] \quad (27b)$$

$$\omega_r \ll \frac{1}{2} kv_o. \quad (27c)$$

The dispersion relationship (26) appears to be new. To gain some understanding, we derive it simply as follows. Upon dropping B_{1i} in Eq. (4), we obtain

$$\gamma m_e \ddot{\xi}_e = - |e| [E_{1e} + (v_o/c) B_{1e} + E_{1i}]$$

or equivalently

$$- \gamma m_e \Omega^2 \xi_e = - |e| (E_{1e}/\gamma^2 + E_{1i}) \quad (28a)$$

where we have used the fact that the self field E_{1e} is canceled by the Lorentz force $(v_o/c) B_{1e}$ by the factor $1/\gamma^2$. [cf. Fig. 1]. Again, neglecting E_{1i} in comparison to E_{1e} in (5), we have

$$- m_i \omega^2 \xi_i = |e| E_{1e}. \quad (28b)$$

We now use the expressions $E_{1e} = 4\pi |e| n_b \xi_e$ and $E_{1i} = -4\pi |e| n_p \xi_i$ in (28a) and (28b). The dispersion relation

$$1 - \frac{\omega_{b11}^2}{\Omega^2} = \frac{\omega_p^2 \omega_{b1}^2}{\omega \Omega^2} \quad (29)$$

is then readily obtained from (28a), (28b). Aside from the factor β^2 (which has been assumed to be closed to unity in this subsection), Eq. (29) is identical with (26). This simple derivation may be used to provide a physical explanation of the instability, similar to that given in Fig. 3. Note that while this derivation is very similar to that given for the hybrid mode, the scalings of the growth rates for the two instabilities are different [cf. Figs. 2, 8; Eqs. (13), (26)].

$$(B3) \quad 1/\beta^2 \gamma^2 < \eta < \beta^2 \gamma^2 \quad (\text{DOMAIN V})$$

The remaining domain is $1/\beta^2 \gamma^2 < \eta < \beta^2 \gamma^2$. This is labeled as Domain V in Fig. 4. The dominant instability for this parameter space is the hybrid mode studied in detail in Section II. The simple dispersion relation was given by Eq. (13) and sketched in Fig. 2 of that section. We note, from the simple derivation given in Sec. II, that this domain is characterized by $\gamma \gg 1$ and $\omega_{b1}^2/\omega_p^2 \gg 1$ [cf. Eqs. (1) and (14)]. The condition $\omega_{b1}^2/\omega_p^2 \gg 1$ is just $\eta \gg 1/\beta^2 \gamma^2$ when $\beta \rightarrow 1$.

Finally, we note that the classification shown in Fig. 4 is symmetrical about $\eta = 1$. This is reasonable if one views the beam plasma interaction in a frame moving at the mean speed of the two species. We also stress that the simple dispersion relations given for Domains (I) - (V) are strongly supported by the numerical computation of the full dispersion relationship (15).

IV. Some Examples

In this section, we give a few examples on the use of the classification schemes. These examples are drawn from laser accelerations of ultra-high

energy particles,^{2,3} the plasma assisted injection and extraction of electrons into a modified betatron.⁷ The simple formula and Fig. 4 provide ready characterization of the instability, in terms of the growth rate and the critical axial wave number (above which the system is stable). One example is given to each of the Domains III, IV, V. [Domains I and II cover the more familiar plasma interactions with a non-relativistic electron beam, and will not be considered further in this section].

A. Laser Beat Wave Acceleration²

Consider the acceleration of an electron beam whose energy is 10 MeV. Let r_b = beam radius = 0.5 mm., I_b = beam current = 0.1A. This beam is embedded in a background hydrogen plasma, of density $n_p = 10^{16}/\text{cm}^3$, say.³ These parameters yield $\gamma = 20.6$, $\omega_p = \omega_{pe} = 5.64 \times 10^{12}$ rad/sec., $\omega_{b11} = 3.11 \times 10^7$ rad/sec, $\omega_{b\perp} = 6.4 \times 10^8$ rad/sec. Then $\eta = \omega_{b11}^2/\omega_p^2 = 3.03 \times 10^{-11}$ which is much less than $1/\gamma^2\beta^2 = 2.36 \times 10^{-3}$. Thus the parameters lie within domain III.

The growth rates and critical wave numbers may be evaluated using Eqs. (23). We arbitrarily take $k_{\perp} = 1/r_b$. Then (24) yields $\bar{\eta} = \eta k_{\perp}^2 c/\omega_p = 0.106\eta = 3.22 \times 10^{-12}$. Thus, Eq. (23) yields $\omega_i = 2.03 \times 10^9 \text{ sec}^{-1}$. For a pulse length $\tau_p = 3.33 \times 10^{-10}$ sec, $\omega_i \tau_p = 0.68$, which is the total number of e-folds during the beam pulse. Thus, the instability is very mild. The half wavelength at k_c is $\lambda_c/2 = \pi/k_c = 0.017$ cm, according to (23b).

The instability growth rates [cf. (23a)] is proportional to the 1/3 power of I_b/γ . Thus the conclusion given in the previous paragraph regarding the unimportance of the instability remains valid for a substantially higher beam current, or at a higher beam energy.

B. Plasma Assisted Injection of Electron Beam in a Modified Betatron Configuration

The modified betatron configuration⁶ consists not only of the usual betatron magnetic field but also a strong toroidal magnetic field. To inject an electron beam into the modified betatron, it is proposed to create a plasma channel⁷ into which the electron beam propagates. In the ion focus regime,

$$\omega_p = \omega_{pi}.$$

To determine the extent of the beam ion interaction, consider, for example, an electron beam of energy 1 MeV, of beam current 1 KA and beam radius of 0.5 cm. Then $\beta = 0.941$, $\gamma = 2.957$, $n_b = 2.7 \times 10^{11}/\text{c.c.}$, $\omega_{b||} = 5.7 \times 10^9 \text{ rad/sec.}$, $\omega_{b\perp} = 1.69 \times 10^{10} \text{ rad/sec.}$ If the ion channel is formed by benzene gas, $m_i = 78 \times 1840 m_e$. Take $n_i = n_e$, then $\omega_p = \omega_{pi} = 7.4 \times 10^7 \text{ rad/sec.}$ Thus $\eta = \omega_{b||}^2 / \omega_p^2 = 5.8 \times 10^3$. Together with $E_b = 1 \text{ MeV}$, we note that the parameters lie within Domain IV [cf. Fig. 4]. If we arbitrarily take $k_{\perp} = 1/r_b$, then $k_{\perp}^2 c^2 > \omega_p^2 + \omega_{b\perp}^2$ and the dispersion relation (26) is a good approximation to (25).

The growth rate and k_c are given by Eqs. (27a) and (27b). Using the parameters given in the previous paragraph, we deduce $\omega_i = 4.3 \times 10^8 \text{ sec}^{-1}$, so that during the time scale $\tau_p = 20 \text{ ns}$, say, corresponding to a single turn injection time of the NRL modified betatron,¹⁵ the total number of e-folds of the instability is $\omega_i \tau_p = 8.6$. This suggests that the beam type Weibel mode may be marginally important since the above analysis excludes stabilizing influence such as betatron oscillation, external magnetic field, random ion motion,¹⁷ the anharmonic property of the channel, and the convective nature of the mode. Thus, the total number of e-folds is expected to be somewhat less than 8.6, and, as a result, be tolerable. From (27b), we have $\lambda_c/2 = \pi/k_c = 13.4 \text{ cm}$. This provides an estimate of the axial extent of the mode.

C. Plasma Assisted Extraction of Electron Beam in a Modified Betatron Configuration

The idea of using a plasma channel may also be adopted for the extraction of an electron beam, after the latter has completed the acceleration phase in a modified betatron configuration.⁷ Note that such an idea is especially attractive for beam extraction, because the contamination of the chamber would not become an issue.

To determine the interaction between the post-accelerated beam and the channel ions, consider, again, an electron beam of current 1 KA, beam radius $r_b = 0.5$ cm, this again yields $n_b = 2.7 \times 10^{11}$ /c.c. If benzene is used, and if $n_i = n_b$, then $\omega_p = \omega_{pi} = 7.4 \times 10^7$ rad/sec as in Subsection IV B. If the energy of the beam is about 50 MeV, say, ($\gamma = 100$), then $\omega_{b||} = 2.9 \times 10^7$ rad/sec and $\omega_{b\perp} = 2.9 \times 10^9$ rad/sec. The parameter $\eta = \omega_{b||}^2 / \omega_p^2 = 0.152$. These values of (E_b, η) lie within Domain V in Fig. 4. Thus, the post-accelerated beam is subject to the hybrid mode.

The growth rate and k_c for the hybrid mode are given by (11). Using the above parameters, we have $\omega_i = \omega_p \omega_{b\perp} = 4.6 \times 10^8$ sec⁻¹. This growth rate is similar to that in Subsection B. However, here $\lambda_c/2 = \pi/k_c = 1$ m, which is quite long. In fact, for parameters similar to the NRL modified betatron, the length of the channel is always less than 60 cm, by geometrical considerations. The relatively mild growth and, more importantly, the long wavelength nature of the hybrid mode, render this method of beam extraction attractive.

V. Discussions

In this paper, we classify beam plasma interaction according to just two parameters: the beam energy and the beam-plasma density ratio. The dispersion relationship is fully electromagnetic and fully relativistic, and

has been given by various authors. Here, we divide the parameter space into several domains, in each of which the instability growth rate and axial scale lengths are simply given. We stress the simplicity, the exposition of the instability mechanism, and the ease with which such a classification may be applied to a particular situation. Examples are given.

While the classification given in this paper provides an immediate assessment of the instability growth rates ---- over a wide range of beam energy and of number densities, the following limitations should be kept in mind. (a) The role of external magnetic fields have been ignored. In the ion focus regime, this assumption may be argued to be valid. However, in many other cases, this assumption cannot be made and the classification given here can no longer be used. Intuitively, the magnetic field may be ignored if $\Omega_j^2 \ll \omega_j^2$, where Ω_j and ω_j are respectively the relativistic cyclotron frequency and the relativistic plasma frequency of the j^{th} species. (b) Perhaps equally restrictive is our over-simplification of the equilibrium fields. The influence of the self fields on this classification remains to be determined. (c) When the densities are high, collisional effects, which have been neglected in this paper, may become important. (d) We have ignored betatron oscillations of the beam electrons, and possible ionic motions in the unperturbed states. These effects are likely to be stabilizing. (e) We have not characterized the absolute or convective behavior of the instabilities. From previous experience with beam instabilities, we anticipate that the instability is mildly absolute, whose time asymptotic response behaves like $\exp(t^a)$, where $0 < a < 1$, typically. However, inclusion of betatron oscillations would tend to make the instabilities convective.⁹ (f) We conjecture that the details of the beam profiles are not very crucial in the classification of beam instabilities. Experience suggests that the radial

scale length of the beam provides a convenient estimate for k_{\perp}^{-1} . The details would be less important.⁹⁻¹¹ Incidentally, in the classical two stream instability, the presence (or absence) of discrete modes depends on the sharpness of the boundaries. However, the time asymptotic response is just equal to that associated with the highest local growth, regardless of the profile.^{9,16}

Finally, we comment on a few works on electron-ion instabilities. Manheimer¹⁷ provided a detailed calculation with the use of a self-consistent equilibrium distribution for the ions. However, the electron inertia, which is extremely important for the hybrid mode, is neglected (justifiably because of the strong magnetic field he assumed). Buchanan¹⁸ includes the electron inertia, but apparently he ignored the possible cancellation, between the E_{1e} and $(v_o/c)B_{1e}$, to order $1/\gamma^2$, as explained in Sec. II and Subsection IIIb. Davidson and Uhm¹⁹ included the case of a strong magnetic field, and Uhm²⁰ recently concluded that two stream instabilities are unimportant for highly relativistic beams. Godfrey²¹ and his coworkers performed particle simulations in the ion focus regime. None of these authors gave the hybrid mode nor the classification,²² as stressed in the present paper.

Acknowledgment

I am grateful to M. Lampe, P. Sprangle, B. H. Hui, W. M. Manheimer, G. Joyce and C. Kapetanakos for many helpful discussions. This work was supported by the Office of Naval Research and the Defense Advanced Research Projects Agency under ARPA Order Number 4395, Amendment No. 41, and monitored by Naval Surface Weapons Center.

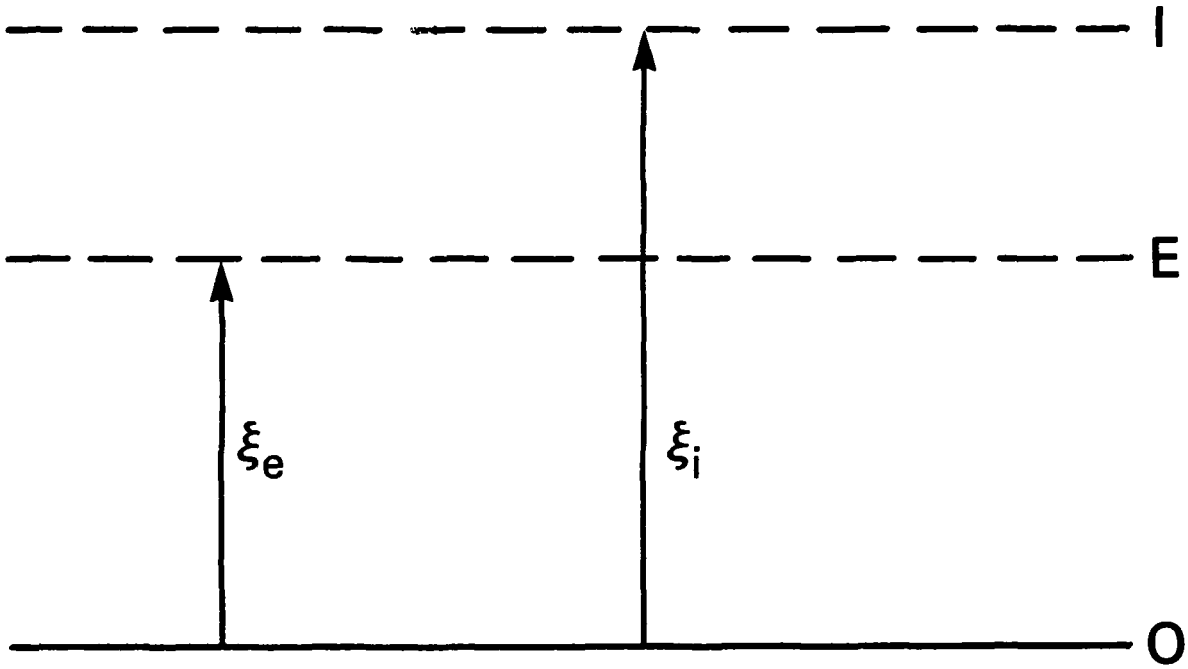


Fig. 1 — Electron sheet E and ion sheet I displaced from their equilibrium position O.

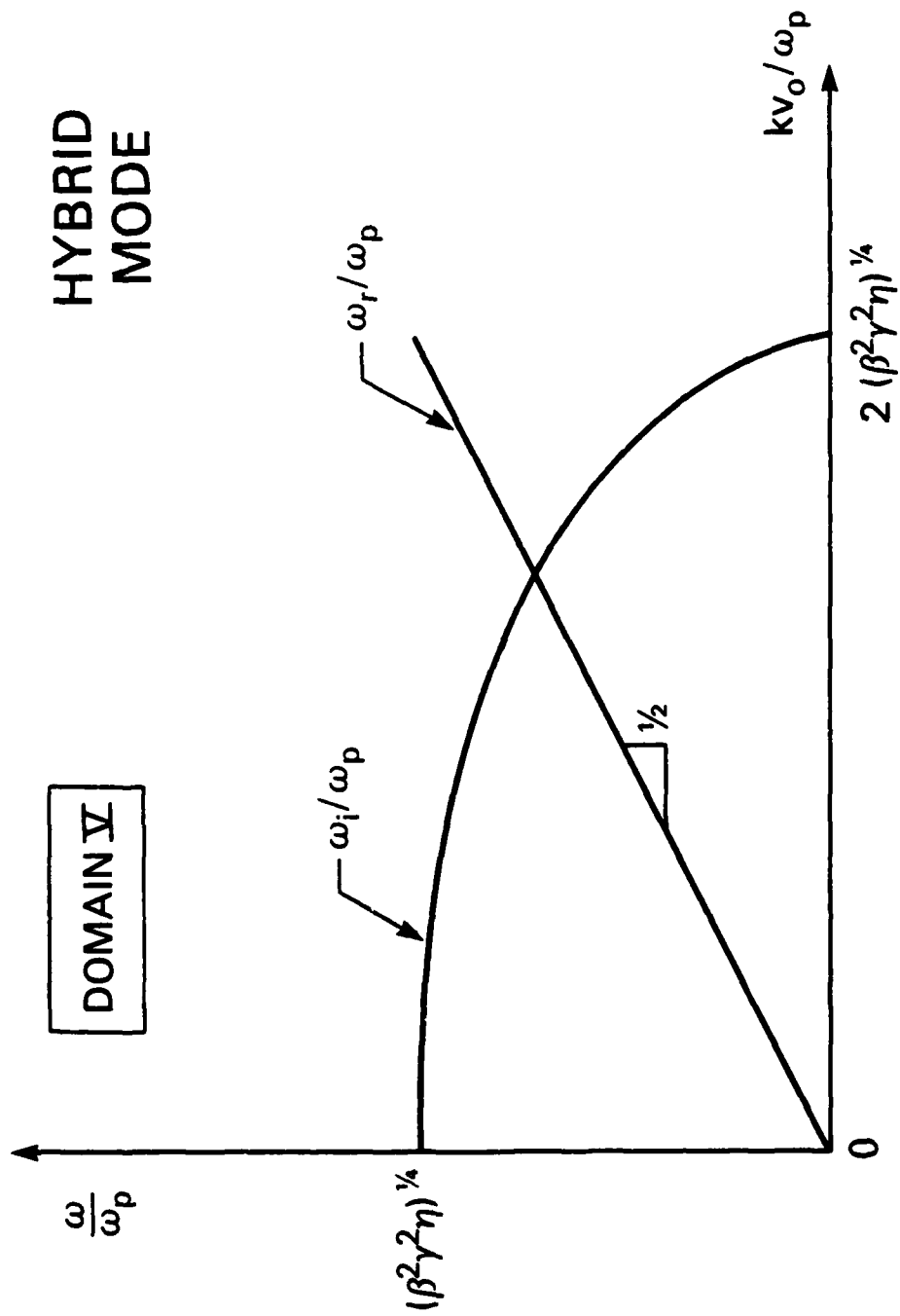


Fig. 2 — Normalized (complex) frequency as a function of the normalized axial wave number for the hybrid mode. See Fig. 4 for the label Domain V.

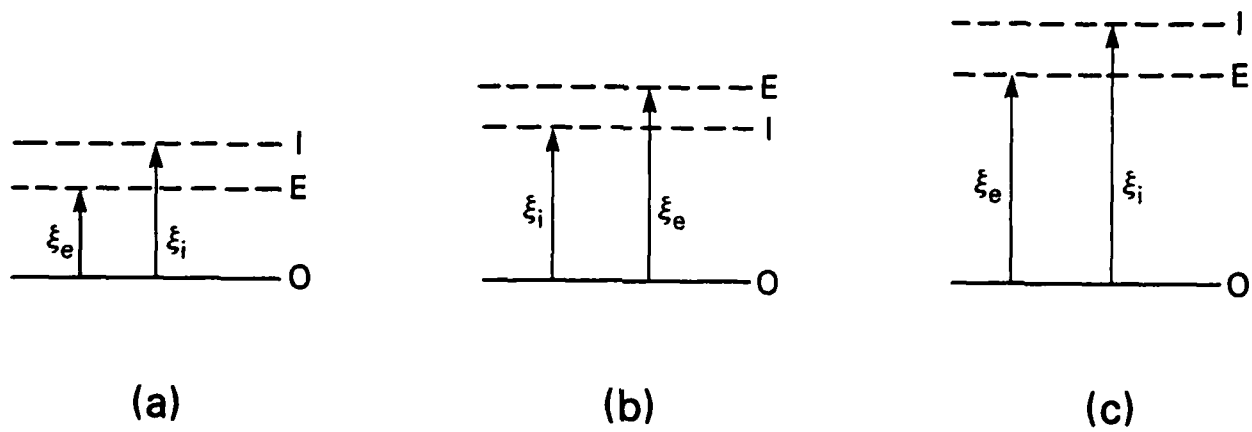


Fig. 3 — Instability mechanism for the hybrid mode.

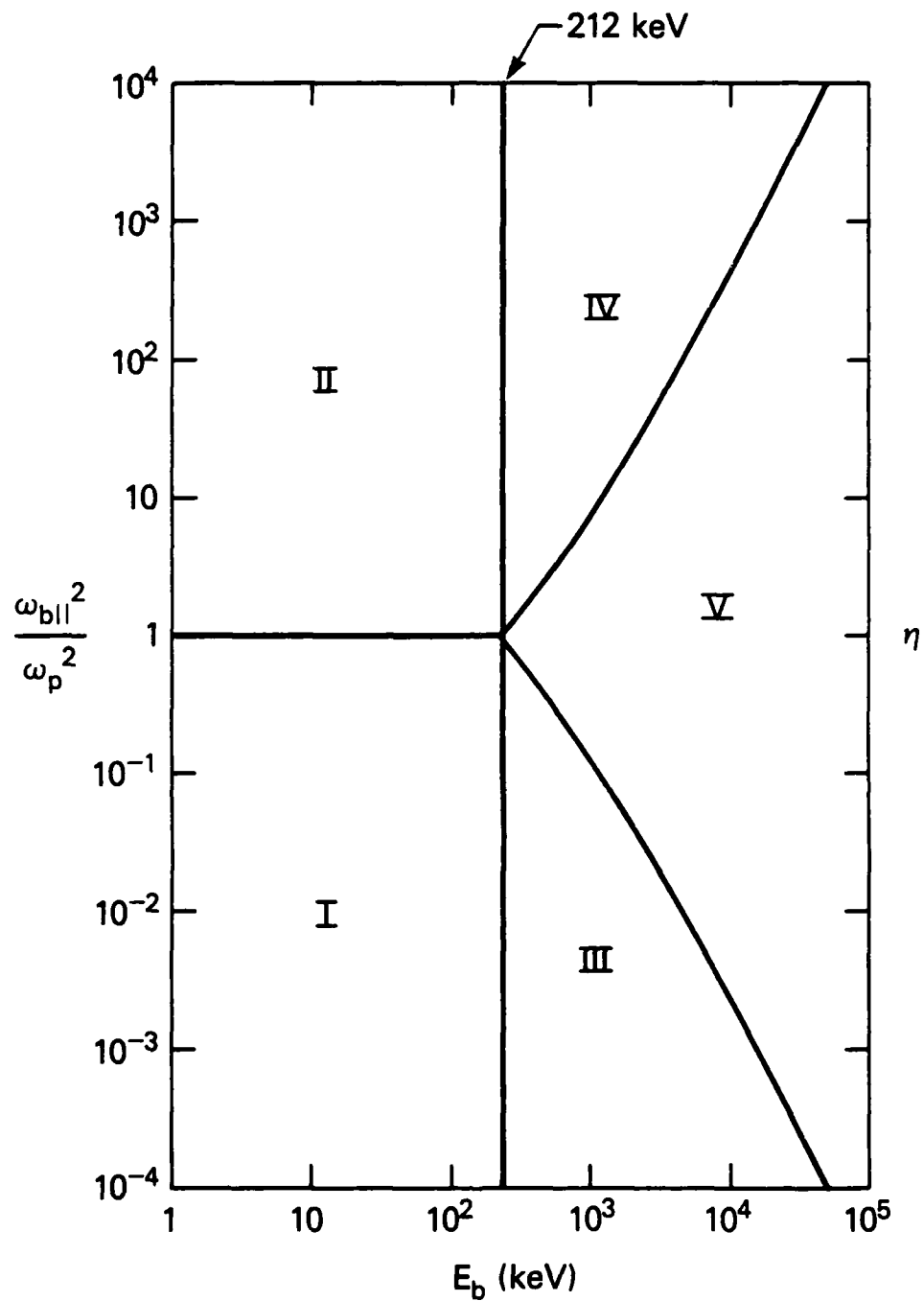


Fig. 4 — Classification of beam plasma interaction. On the boundary between Domain IV and V, $\eta = \beta^2\gamma^2$; and on that between III and V, $1/\eta = \beta^2\gamma^2$.

DOMAIN I

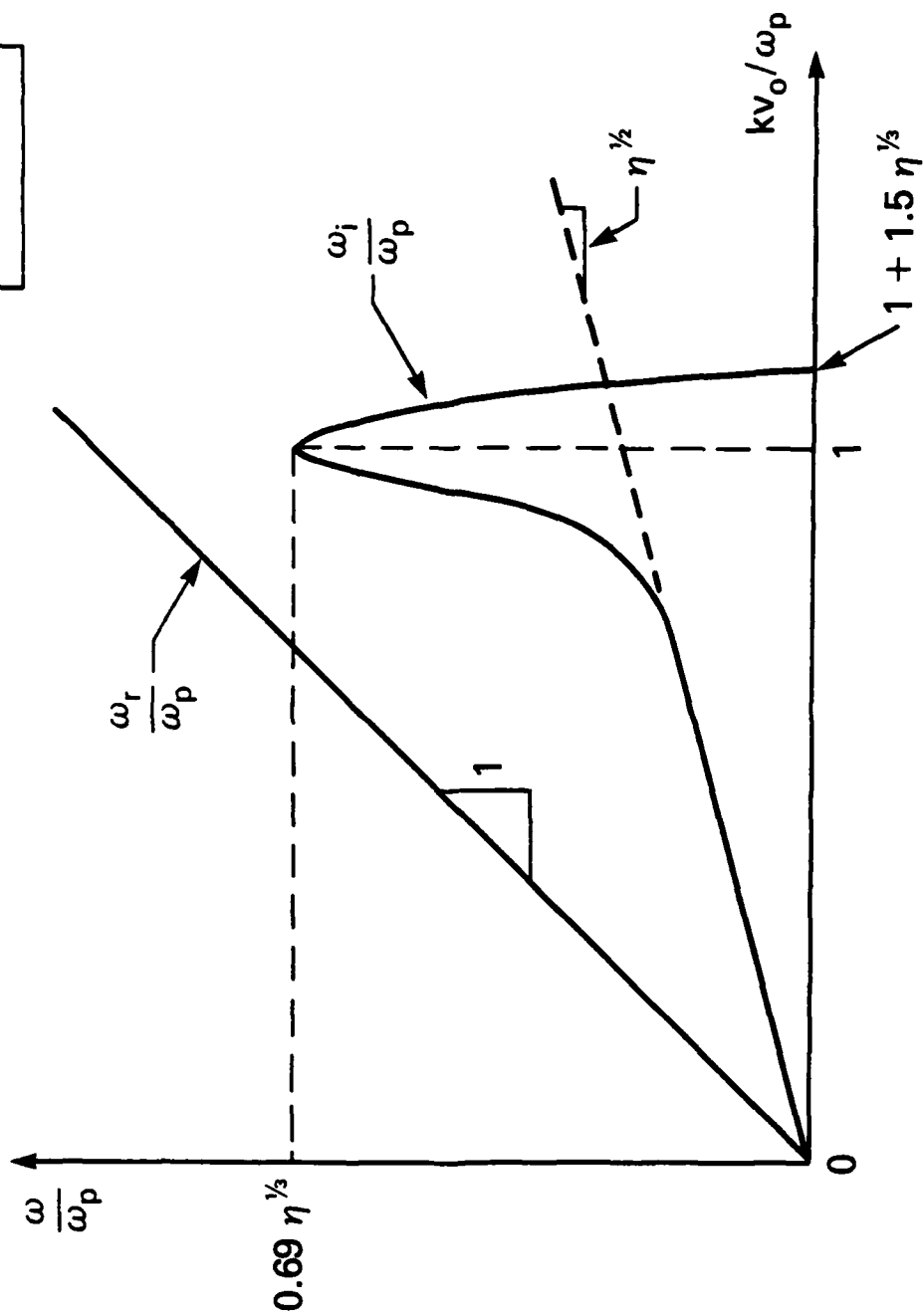


Fig. 5 — The normalized (complex) frequency as a function of the normalized axial wave number, for Domain I of Fig. 4.

DOMAIN II

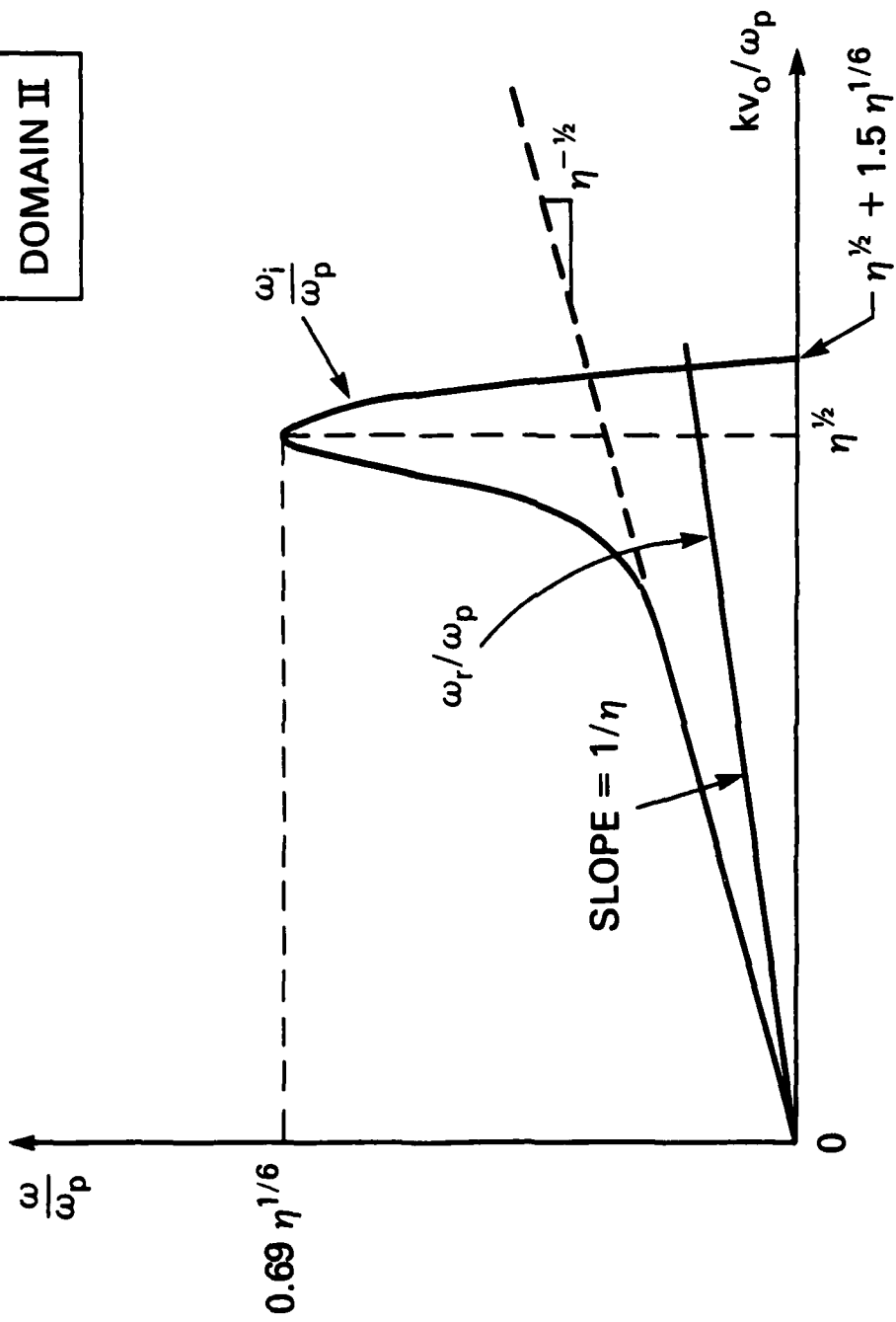


Fig. 6 — As in Fig. 5, for Domain II of Fig. 4.

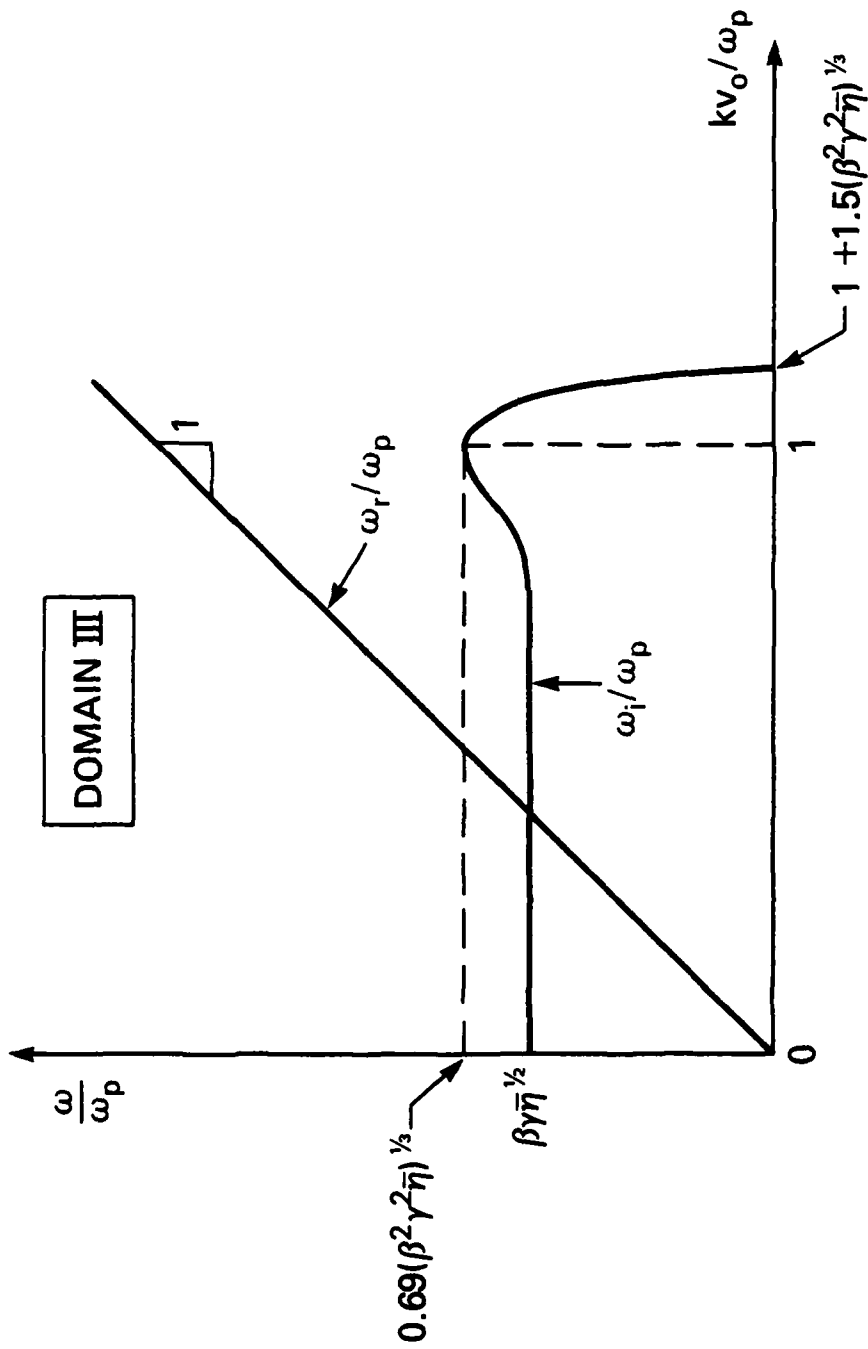


Fig. 7 — As in Fig. 5, for Domain III of Fig. 4.

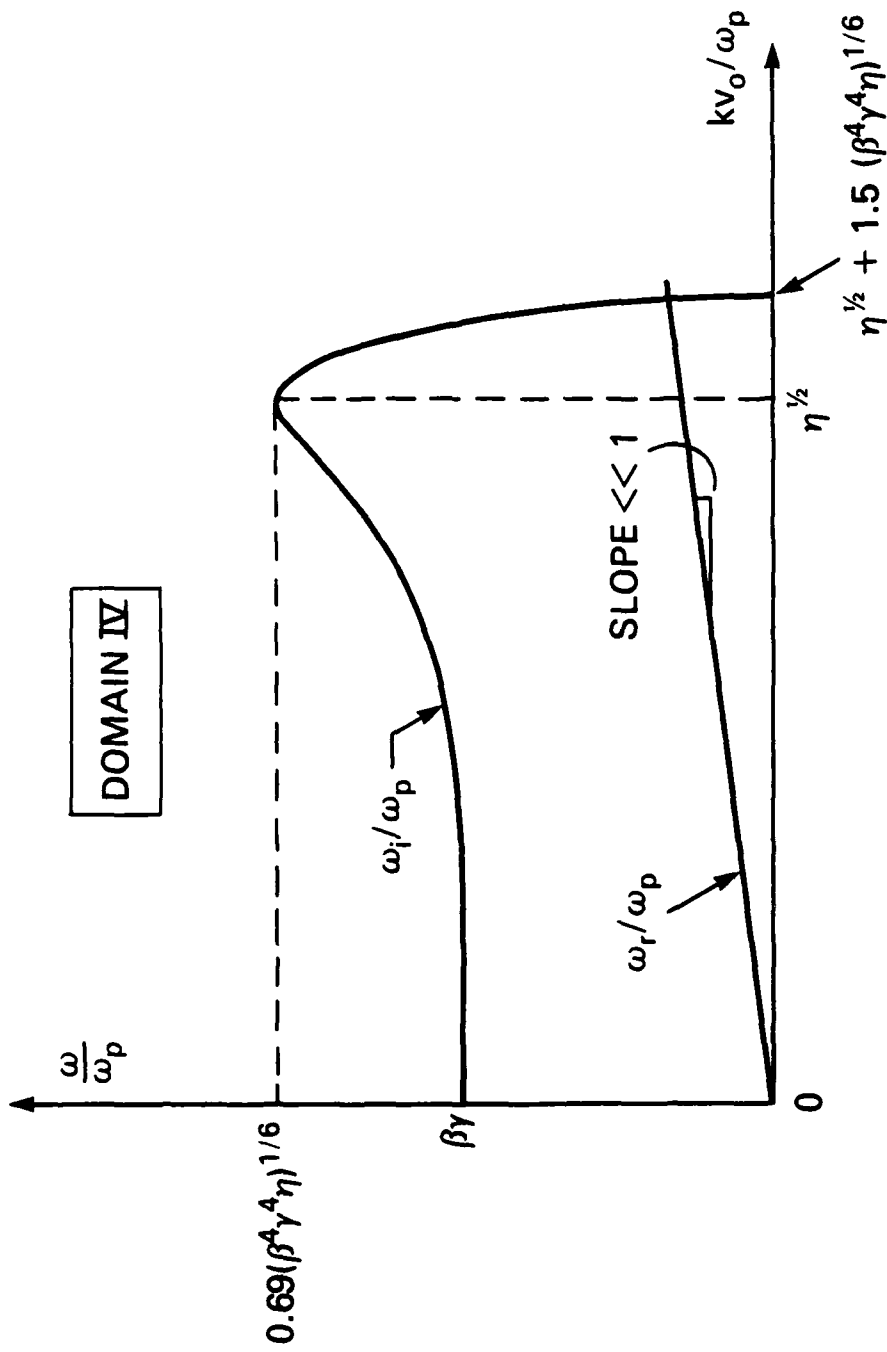


Fig. 8 -- As in Fig. 5, for Domain IV of Fig. 4.

Appendix HYBRID MODE IN A FINITE BEAM

In this appendix, we consider in some detail the interaction between a relativistic electron beam, of radius r_b , and a background plasma, the latter being infinite in extent. We focus on the hybrid mode. We show that the growth rate given by Eq. (13) is also applicable when the beam is finite. This study provides additional confidence in the replacement of k_{\perp} by p/r_b , where p is some quantized number of order unity, or higher.

When the equilibrium self fields are ignored, the interactions of the electron beam and a cold background plasma are described by the following coupled differential equations:¹¹

$$\frac{1}{r} \frac{d}{dr} \left\{ \frac{r\zeta}{\delta} \frac{dE_z}{dr} \right\} - \frac{\ell^2}{r^2} \frac{\zeta}{\delta} E_z - \epsilon E_z = \frac{i\ell B_z}{r\kappa^2} \frac{d\rho}{dr} \quad (A1)$$

$$\frac{1}{r} \frac{d}{dr} \left\{ \frac{r}{\delta} \frac{dB_z}{dr} \right\} - \frac{\ell^2}{r^2} \frac{B_z}{\delta} - B_z = \frac{-i\ell E_z}{r\kappa^2} \frac{d\rho}{dr}. \quad (A2)$$

Here, E_z and B_z are the rf field components of the TM and TE modes, which are coupled if the azimuthal mode number $\ell \neq 0$. Small signal dependence of the form $f(r) \exp(i\omega t - i\ell\theta - ikz)$ has been assumed. The symbols in (A1) and (A2) are defined as

$$\kappa^2 = k^2 - \omega^2/c^2; \quad \delta = k^2 - \omega^2/c^2 + (\omega_p^2 + \omega_{b\perp}^2)/c^2 \quad (A3)$$

$$\epsilon = 1 - \frac{\omega_p^2}{\omega^2} - \frac{\omega_{b\perp}^2}{\Omega^2}; \quad \zeta = \epsilon - \frac{\beta^2 \omega_p^2 \omega_{b\perp}^2}{\omega^2 \Omega^2} \quad (A4)$$

$$\rho = \frac{1}{\delta c^2} \left[\frac{k c \omega_p^2}{\omega} + \frac{\omega_{b\perp}^2 (k c - \omega v_o / c)}{\Omega} \right]. \quad (A5)$$

Consider first a local analysis of (A1). Take $l = 0$ for convenience and replace d/dr by $-ik_{\perp}$. Then Eq. (A1) yields

$$-k_{\perp}^2 \zeta / \delta - \epsilon = 0 \quad (A6)$$

which can easily be shown to be the dispersion relationship (15). It is also quite clear that, in general, $1/r_b$ provides a natural transverse scale length of the perturbations. In fact, one may use a normalized variable $x = r/r_b$ to render (A1) and (A2) dimensionless.

For general l , and for a constant beam density up to $r = r_b$, (and zero for $r > r_b$), a transcendental dispersion relationship,¹¹ in terms of Bessel functions, may be obtained from (A1) and (A2). This dispersion relationship may be obtained by requiring that E_z and B_z be continuous at $r = r_b$, but E_z' and B_z' be discontinuous by an amount which is to be computed from an integration of (A1) and (A2), due to a discontinuity in ρ . This dispersion relationship may be simplified considerably under the assumption

$$\omega_{b11}^2, \omega_p^2 \ll \omega^2, \Omega^2 \ll \omega_{b\perp}^2 \ll \frac{c^2}{r_b^2}. \quad (A7)$$

In this case, it reads

$$J_l(\tilde{\beta}) = 0 \quad (A8)$$

where

$$\tilde{\beta} = \frac{i\omega_{b\perp} r_b / c}{\sqrt{1 - \frac{\omega_p^2 \beta^2 \omega_{b\perp}^2}{\Omega^2 \omega^2}}} = \lambda_{\ell\nu} \quad (\text{A9})$$

and $\lambda_{\ell\nu}$ is the ν -th zero of the Bessel function J_ℓ . To the lowest order in $\omega_{b\perp} r_b / c$ [cf. (A7)], (A9) then yields

$$1 - \frac{\omega_p^2 \beta^2 \omega_{b\perp}^2}{\Omega^2 \omega^2} = 0. \quad (\text{A10})$$

The solution to (A10) is

$$\omega = \frac{1}{2} k v_o \pm i \left(\beta \omega_p \omega_{b\perp} - \frac{1}{4} k^2 v_o^2 \right)^{1/2} \quad (\text{A11})$$

which is just the dispersion relation (11) for the hybrid mode [aside from the factor β , which has been assumed to be closed to unity in the derivation of (11)]. The dispersion relationship (A11) is sketched in Fig. 2.

Finally, we remark that as long as (A7) is valid, the growth rate given by the local analysis is anticipated to be valid also for a diffuse beam profile. This has also been pointed out by Tajima.¹⁰

References

1. L. E. Thode, Los Alamos Scientific Laboratory Report No. LA-7715-MS, (1980).
2. T. Tajima and J. M. Dawson, Phys. Rev. Lett. 43, 267 (1979).
3. C. M. Tang, P. Sprangle and R. N. Sudan, NRL Memo Report 5324 (1985). ADA149688
4. R. J. Briggs, R. E. Hester, E. J. Lauer, E. P. Lee and R. L. Spoerelin, Phys. Fluids 19, 1007 (1976), W. E. Martin, et. al., Phys. Rev. Lett. 54, 685 (1985) and references therein.
5. W. W. Destler, P. G. O'Shea and M. Reiser, Phys. Rev. Lett. 52, 1978 (1984).
6. P. Sprangle and C. A. Kapetanacos, J. Appl. Phys. 49, 1 (1978); also, F. Mako, W. Manheimer, C. A. Kapetanacos, D. Chernin and F. Sandel, NRL Memo Report 5196 (1983). ADA134694
7. B. H. Hui and Y. Y. Lau, Phys. Rev. Lett. 53, 2024 (1984).
8. B. I. Aronov, L. S. Bogdankevich and A. A. Rukhadze, Plasma Phys. 18, 101 (1976).
9. R. J. Briggs, in Advances in Plasma Physics, edited by A. Simon and W. B. Thompson (Interscience, New York, 1971).
10. T. Tajima, Phys. Fluids 22, 1157 (1979).
11. M. E. Jones, Phys. Fluids 26, 1928 (1983).
12. M. M. Shoucri, Phys. Fluids 26, 3096 (1983).
13. E. S. Weibel, Phys. Rev. Lett. 2, 83 (1959).
14. See also Eq. (42) of Ref. 10.
15. C. A. Kapetanacos, P. Sprangle, D. P. Chernin, S. J. Marsh and I. Haber, Phys. Fluids 26, 1634 (1983).
16. E. A. Frieman, M. L. Goldberger, K. M. Watson, S. Weinberg and M. N. Rosenbluth, Phys. Fluids 5, 196 (1962).
17. W. M. Manheimer, Part. Accelerators 13, 209 (1983).

18. H. L. Buchanan, Lawrence Livermore National Laboratory, Report Nos. UCID-19495, and 19675 (1982).
19. R. C. Davidson and H. S. Uhm, J. Appl. Phys. 51, 885 (1980).
20. H. S. Uhm, to be published.
21. B. Godfrey, private communication.
22. Y. Y. Lau, Bull. Am. Phys. Soc. 29, 1349 (1984).